 doi:10.20944/preprints202010.0645.v1

Article

Tailoring of thermo-mechanical properties of hybrid composite-metal bonded joints

Tasnuva Khaleque [1], Xialong Zhang [2], Vijay Kumar Thakur [3], Indrat Aria [4] and Hamed Yazdani Nezhad [1,*]

[1] Department of Mechanical Engineering and Aeronautics, City University of London, London EC1V 0HB, UK
[2] Enhanced Composites and Structures Centre, Cranfield University, Milton Keynes MK43 0AL, UK
[3] Department of Engineering, Science and Technology, SRUC, Edinburgh DG1 3NE, UK
[4] Surface Engineering Precision Institute, Cranfield University, Milton Keynes MK43 0AL, UK
* Correspondence: hamed.yazdani@city.ac.uk; Tel.:+44-2070-40506

Abstract: Metallic substrates and polymer adhesive in composite-metal joints have a relatively large coefficient of thermal expansion (CTE) mismatch, which is a barrier in the growing market of electric vehicles and their battery structures. It is reported that adding carbon nanotubes (CNTs) to the adhesive reduces the CTE of the CNT enhanced polymer adhesive multi-material system, therefore when used in adhesively bonded joints it would, theoretically, result in low CTE mismatch in the joint system. The current article presents the influence of two specific mass ratios of CNTs on the CTE of the enhanced polymer. It was observed that the addition of 1.0 wt% and 2.68 wt% of multi-walled CNTs (MWCNTs) decreased the CTE of the polymer adhesive from $7.5 \times 10^{-5}\ ^{\circ}C^{-1}$ (pristine level) to $5.87 \times 10^{-5}\ ^{\circ}C^{-1}$ and $4.43 \times 10^{-5}\ ^{\circ}C^{-1}$, respectively by 22% and 41% reduction. The reduction in the CTE was predicted, theoretically, which showed that CTE should have been reduced to $3.6 \times 10^{-5}\ ^{\circ}C^{-1}$ (52% reduction) and $1.4 \times 10^{-5}\ ^{\circ}C^{-1}$ (81% reduction). This may be due to the fact that, Raman spectroscopy of the MWCNTs identified defects in the raw material, and scanning electron microscopy (SEM) identified agglomeration of MWCNTs on the surface and cross-section of the modified polymers.

Keywords: Composite-metal joint, electric vehicles, carbon nanotubes, polymer adhesive, thermal strain measurement, coefficient of thermal strain mismatch

1. Introduction

Due to their advantages of energy saving and environmental protection, high performance electric vehicles are under rapid development [1]. The structure adhesive bonding technology, as a new type of lightweight structural joining technology nowadays, has a good performance to join dissimilar materials, such as those identified in and solves the technical bottlenecks in conventional joining processes [2–4]. Moreover, it has good sealing and fatigue resistance compared to traditional joining methods, which make them suitable in the assembling process of high-performance electric vehicles [5]. For example, the adhesive bonding technology is applied in the battery pack system, which is one of the core components of the electric vehicles to determine the mileage and speed of the electric vehicles [6]. The disadvantage of this battery pack system is that the batteries discharge at different rates during use, and generate significant heat at different rates of heat generation. Besides, the accumulation of time and space effect will accumulate heat. The temperature in the battery pack area can reach up to $200^{\circ}C$ [7]. The high temperature may lead to significant thermal expansion and residual stress in the battery compartments, resulting in failure of composite-metal bonded joints. The joint failures in the battery pack system will result in some serious problems, such as cracks in joints and moisture in the air enters the battery [5], thus reducing the performance of the battery, and even leading to the failure

Preprints (www.preprints.org) | NOT PEER-REVIEWED | Posted: 30 October 2020 doi:10.20944/preprints202010.0645.v1

of the entire battery pack system, potentially leading to traffic accidents. The main factor impacting the failure of the bonding joint is the coefficient of thermal expansion (CTE) mismatch among components of the joint, especially between the metal and polymer adhesives. The CTE mismatch is the main source of inducing internal shear stress that may result in the joint failure at high temperature. In some studies, it was reported that the carbon nanotubes (CNTs) can be added to the epoxy-based adhesive to adjust the CTE of the enhanced adhesive, therefore adhesives with different CTEs can be produced for various requirements [8].

The present study investigates how the addition of varying weight percentages of CNTs in adhesive affects the CTE of the adhesive in adhesively bonded aluminium - epoxy polymer joints.

2. Experimental Approach

2.1. Materials

A low viscosity bisphenol-A epoxy resin, Araldite LY1564 (Hunstman, UK), was used in the present study. The epoxy was cured using a hardener, Aradur 3486 (Hunstman, UK). The mix ratio of Araldite LY1564 and Aradur 3486 was 100 : 34 by weight. The recommended working temperature of the epoxy system is up to $120^{\circ}C$ [9].

The epoxy was modified with varying weight percentages of multi-walled CNTS (MWCNTs). The weight percentages of MWCNTs used were 1.0 wt% and 2.68 wt%.

A surfactant, Triton X-100, was used to facilitate the dispersion of MWCNTs. The critical micelle concentration (CMC) of Triton X-100 is from 0.22 to 0.24 mM [10] and the molecular weight is 625. So, the CMC is 0.14 mg/ml by weights. When the concentration of Triton X-100 is higher than the CMC, micelles of Triton X-100 occur in the solution, and they further contribute to the dispersion quality of CNTs [11]. The concentration of Triton X-100 used in the present case was ten times of CMC.

2.2. Preparation and Manufacturing

The epoxy adhesive specimens with CNTs and adhesive-metal bonded specimens with CNTs were prepared. Aluminium (Al) was used as substrates for adhesive-metal bonded specimens. Five types of specimens were manufactured as shown in the Table 1 and Figure 1.

Table 1. List of specimens manufactured in the present study

Specimen	Constitution	Dimension
Specimen a	epoxy+Al+1.00 % CNTs	Figure 1 (a)
Specimen b	epoxy+Al+2.68 % CNTs	Figure 1 (a)
Specimen c	epoxy+1.00% CNTs	Figure 1 (b)
Specimen d	epoxy+2.68% CNTs	Figure 1 (b)
Specimen e	Al only	Figure 1 (c)

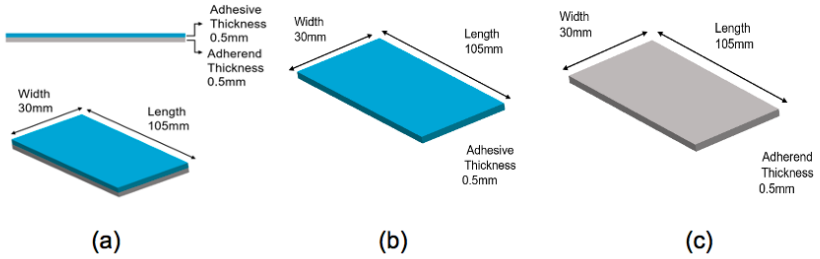

Figure 1. Schematics of specimens manufactured (a) hybrid joint specimen (b) epoxy specimen and (c) aluminium specimen

Preprints (www.preprints.org) | NOT PEER-REVIEWED | Posted: 30 October 2020 doi:10.20944/preprints202010.0645.v1

Firstly, the aluminum substrates were polished with 100-grit grinding paper to make the surfaces chemically active. Within an hour before bonding, 400-grit grinding paper was used to polish to avoid the potential oxidation on the bonding area. Acetone was used to wipe the bonding area to thoroughly clean any remaining contaminants on the surface, so as to ensure good bonding quality and the final performance of the specimens, i.e. ensuring the ultimate bond strength was reached.

The aluminium moulds for the manufacturing of specimens were manufactured as per Figure 2 and Figure 3. The moulds were equipped with release film to avoid the residue of the polymer after curing. The surface treatment using acetone and release agent was also performed before the application of the adhesive. Mould 1 was used to manufacture the specimen a and specimen b. The thickness of the chambers in mould 1 was 1mm; an aluminium substrate with the thickness of 0.5 mm was inserted inside to produce an adhesive thickness of 0.5 mm.

Mould 2 was used to manufacture the specimens c and specimen d; the thickness of the chamber in mould was 0.5 mm to manufacture specimens having 0.5 mm thickness.

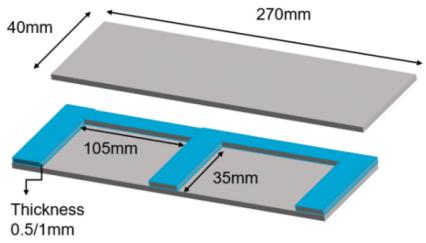

Figure 2. Schematic of the mould manufactured

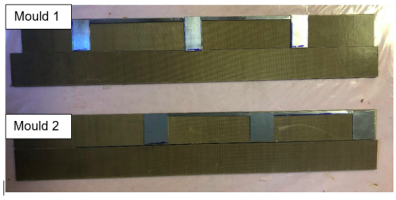

Figure 3. Image of the mould manufactured

The MWCNTs was dispersed in the epoxy/adhesive system using a sonicator. The dispersion process included the following steps:

- weighing, 0.1 gm of CNTs each time
- adding 40 ml of acetone to MWCNTs as the solvent
- sonicating for 30 minutes with 80% amplitude
- gathering all MWCNTs and treating with high shear mixer for 20 minutes
- adding epoxy resin in the solvent
- mixing and evaporating acetone for 5 hours at $80^{\circ}C$

the acetone was evaporated, the curing agent was added to the epoxy resin and MWCNTs mixture. The mixture was then stirred with a spatula and degassed for 30 minutes. The mixture was applied to the mould as an adhesive using a spatula, and the mould was clamped using foldback clips. The mixture was cured at $100^{\circ}C$ for 5 hours. The specimens were taken out from the moulds carefully after curing. The specimens were then trimmed with a cutter knife to remove the residuary side fillets. All specimens were made sure of having approximately identical dimension. Two specimens of each type were manufactured to ensure the accuracy and the repeatability of the results.

Two reflective strips with a length of 10 mm were attached on the surface of the specimen in order to use a laser extensometer. The gap between the two strips was about 50 mm. A thermocouple was attached on the surface of the specimen to monitor its temperature variation.

Preprints (www.preprints.org) | NOT PEER-REVIEWED | Posted: 30 October 2020 doi:10.20944/preprints202010.0645.v1

2.3. Scanning Electron Microscopy

Scanning electron microscopy (SEM) was performed to analyse the dispersion quality of CNTs in the adhesive. Specimen c and specimen d were analysed. One of the two samples from each specimen was analysed for the dispersion of CNTs on the surface of the specimen, the other one was analysed for the dispersion of CNTs on the cross-section of the specimen using a TESCAN LYRA3 microscope.

The specimens were sputter coated with 10 nm gold coating to minimize the charging, and ensure high-quality SEM images from the analysis [12].

2.4. Raman Spectroscopy

The Raman spectroscopy was performed to assess the quality of the CNTs [13]. The amount of defective structures and complete molecular structures were measured, a comparison of the intensity of these two structures provided an evaluation of the quality of the CNTs used as the raw material in the present study. The MWCNTs were dispersed and mixed with silicon oil, the mixture was then loaded with glass slide for the Raman measurement.

2.5. Thermal Strain measurement

The CTE of every specimen was determined using thermal strain measurement technique. A hot-plate was used to attach the specimen onto it, and to heat the specimen up to 120°C at 5°C/min heating rate. A Laser extensometer was used to measure the deformation of the specimen during the heating process. The schematic of the thermal strain measuring system used for the study is shown in Figure 4, and described below:

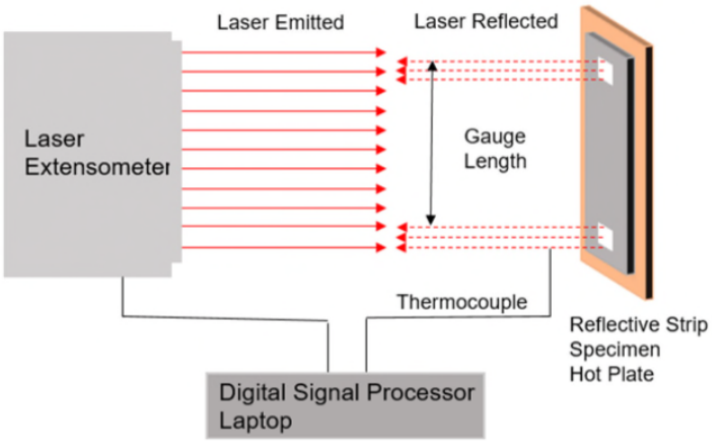

Figure 4. Schematic of thermal strain measurement system

The laser extensometer was positioned at a distance of 305 mm away from the specimen, and was slightly angled (5°C) to avoid the interference from the possible spurious reflections from other reflective surfaces [14]. During the test, the laser emitted from the laser extensometer vertically aimed at the surface of the specimen. The laser extensometer measured and indicated the gauge length between the two reflective strips by the laser reflected from the reflective strips, the gauge length increased with the increase of the temperature. The thermocouple monitored the temperature of the specimen during the test, and the test was stopped when the temperature reached to 120°C to avoid exceeding glass temperature. The digital signal processor transmitted the data to the computer where time, temperature data were recorded using LABVIEW program. The CTE of the specimens was calculated using the following equation:

$$\alpha = \frac{L_{end} - L_{start}}{L_{start} \times (T_{end} - T_{start})} \quad (1)$$

Preprints (www.preprints.org) | NOT PEER-REVIEWED | Posted: 30 October 2020 doi:10.20944/preprints202010.0645.v1

where α is the CTE of the specimen, L_{end} is the gauge length of the specimen at the end of the test, L_{start} is the gauge length at the start of the test, T_{end} is the temperature ($^{\circ}C$) of the specimen at the end of the test, and T_{start} is the temperature ($^{\circ}C$) of the specimen at the start of test.

3. Results

3.1. Fractography

The SEM images in Figures 5-9 show the dispersion quality of the MWCNTs both on the surface and cross-section of the different specimens. In Figures 5 and 6, many MWCNTs protruding out from the surface of cross-section are observed, attributed to the preparation stage where the samples were cut with a scissor, and the cross-section was not polished before gold coating.

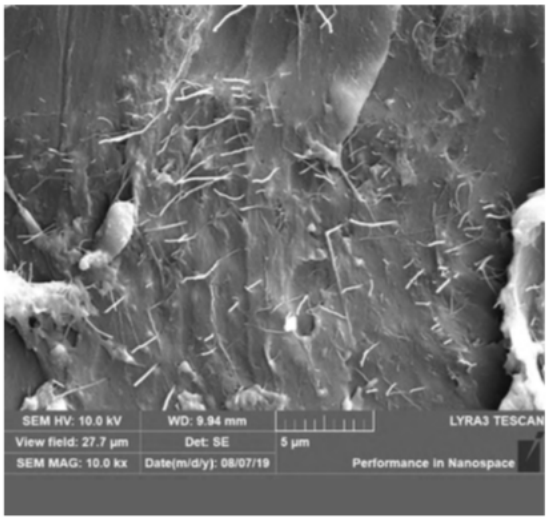

Figure 5. Dispersion of MWCNTs on cross-section of specimen a with 1.0 wt% MWCNTs

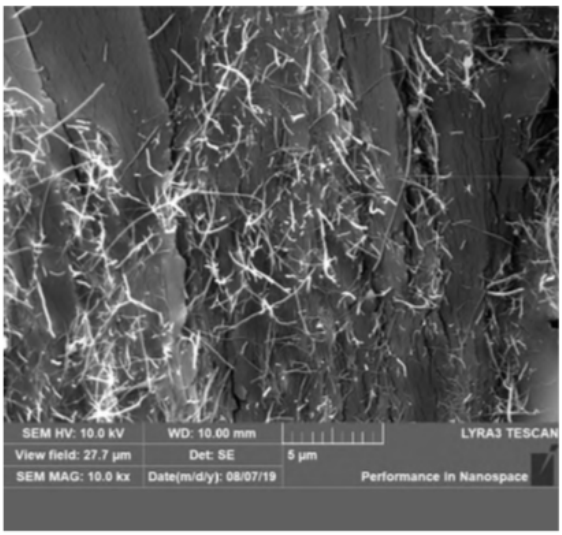

Figure 6. Dispersion of MWCNTs on cross-section of specimen b with 2.68 wt%

Figure 7 shows bundles of MWCNTs (highlighted by red boxes) in specimen c, which are protruding out of the surface, i.e. an obvious agglomeration of MWCNTs was observed. Figure

Preprints (www.preprints.org) | NOT PEER-REVIEWED | Posted: 30 October 2020 doi:10.20944/preprints202010.0645.v1

8 also shows agglomeration on the surface of specimen d (highlighted by red boxes). This indicates that the MWCNTS were poorly dispersed in the polymer possibly due to the re-agglomeration that happened after the curing process.

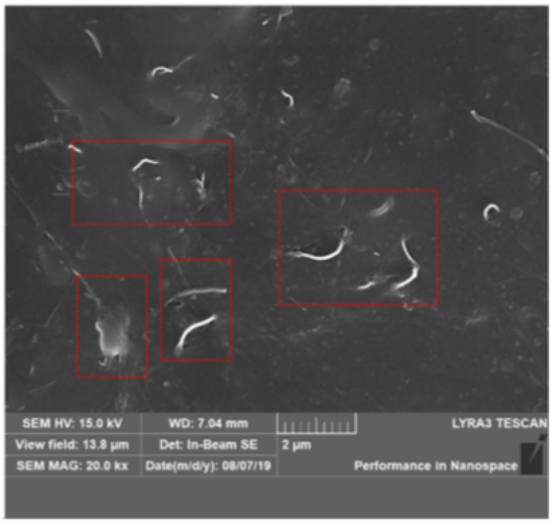

Figure 7. Dispersion of MWCNTs on surface of specimen c with 1.0 wt% MWCTNs

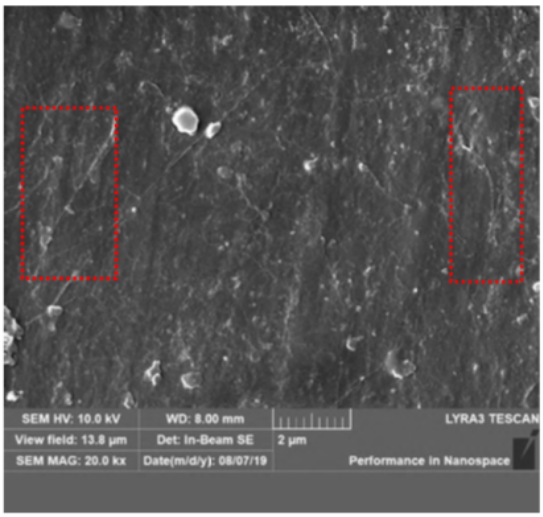

Figure 8. Dispersion of MWCNTs on surface of specimen d with 2.68 wt% MWCTNs

In specimen a and specimen b, the MWCNTs were dispersed well, and no obvious agglomeration occurred as investigated in several SEM images, e.g. see Figure 5 and 6, however, agglomeration is observed in Figure 9 in specimen d. This indicates that the MWCNTs were not well dispersed before application, and hence reagglomeration occurred during the curing process [15]. The high weight percentages of carbon nanomaterials in adhesive was reported as the main reason for agglomeration and change in morphology [16].

Preprints (www.preprints.org) | NOT PEER-REVIEWED | Posted: 30 October 2020 doi:10.20944/preprints202010.0645.v1

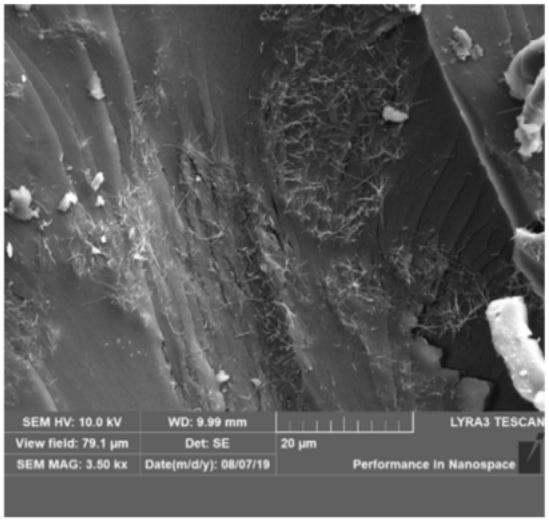

Figure 9. Re-agglomeration of MWCNTs in specimen d

3.2. Raman Spectroscopy

The MWCNTs used in this project were assessed by Raman spectroscopy. Figure 10 shows the evaluation result. The G band corresponds to the order character, and the D band represents the disorder character in Raman spectrum. The intensity of D band was around 1040 and the intensity of the G band was 1270, the intensity ratio of D and G bands, ID/IG was 0.8189. The high intensity ratio indicates that there were a lot of defects in the CNTs. The defects deteriorated the properties of the MWCNTs [13].

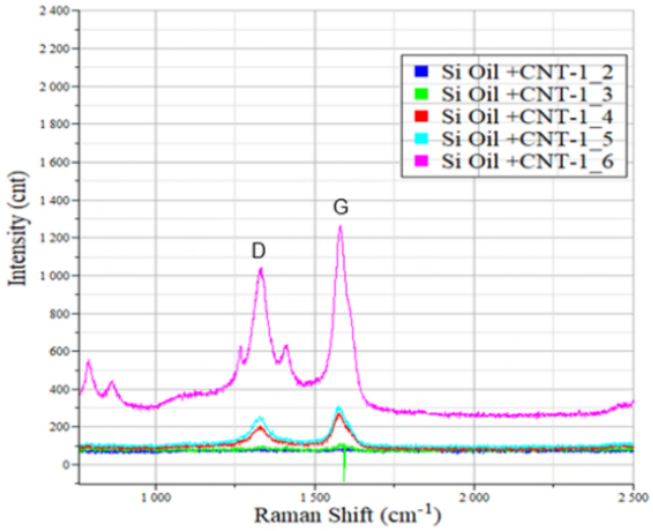

Figure 10. Quality evaluation of MWCNTs

There are two reasons why defects occurred in MWCNTs: the defects may occur during the production process in the lab where the quality was affected by parameters, such as catalyst, temperature, pressure etc. Moreover, the defects of MWCNTs can also be induced during the gathering process from the quartz substrate in our chemical vapour deposition process [17,18].

The second reason is that a large number of defects may occur during the dispersion process, the sonication process and high shear mixing process. It has been reported in the literature that long sonication duration may result in defects in CNTs. The sonication process with lower amplitude and high shear mixing with a lower rotational speed could prevent defects in MWCNTs.

Preprints (www.preprints.org) | NOT PEER-REVIEWED | Posted: 30 October 2020 doi:10.20944/preprints202010.0645.v1

3.3. Coefficient of Thermal Expansion

The gauge lengths of all the specimens were measured with the increase of the temperature. The test started at 30°C and ended at 120°C. The CTE of the specimens were calculated using equation (1) and are listed in Table 2. The comparison of CTEs at different materials, including steel, aluminium, polymer used in the project, and different specimens is shown in Figure 11.

Table 2. Experimentally determined CTEs of five specimens.

Specimen	a	b	c	d	e
Length of thermal expansion (mm)	0.127	0.133	0.257	0.218	0.132
Interval of temperature (° C)	90	90	90	90	90
CTE $\times 10^{-5}$ $^{\circ}C^{-1}$	2.66	2.87	5.87	4.43	2.75

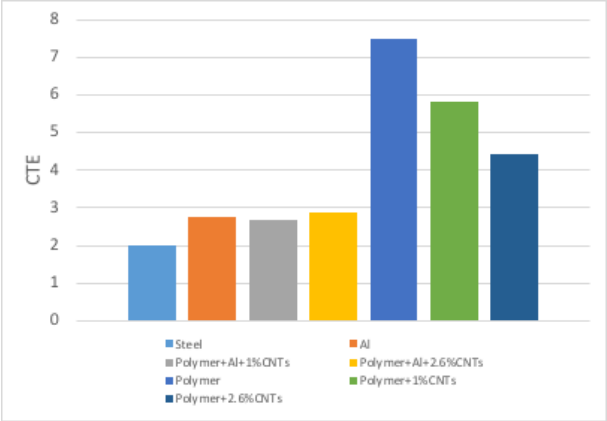

Figure 11. CTE ($\times 10^{-5}$ $^{\circ}C^{-1}$) comparison of different materials and specimens

Figure 11 indicates that the CTEs of hybrid joint specimen a and specimen b, which contain an aluminium substrate, are close to the CTE of the aluminium plate. This is due to the fact that the adhesive and aluminium were bonded together and the bond strength was sufficiently high that the adhesive was forced to expand with the aluminium substrate during the heating process. No disbond was observed after the tests. Besides, due to the CTE mismatch between adhesive and aluminium, the specimen may bend. However, no bending was observed in the test as the thermal strain of the specimen was too small to be observed.

According to the adopted curve in Figure 12 from [8], the CTE of specimen c should be 3.6×10^{-5} $^{\circ}C^{-1}$, and the CTE of the specimen d should be 1.4×10^{-5} $^{\circ}C^{-1}$. However, the results in Table 2 indicate that the CTE of specimen c is actually 5.87×10^{-5} $^{\circ}C^{-1}$ and the CTE of specimen d is 4.43×10^{-5} $^{\circ}C^{-1}$. The difference between the theoretical and the experimental results is attributed to the fact that:

Preprints (www.preprints.org) | NOT PEER-REVIEWED | Posted: 30 October 2020 doi:10.20944/preprints202010.0645.v1

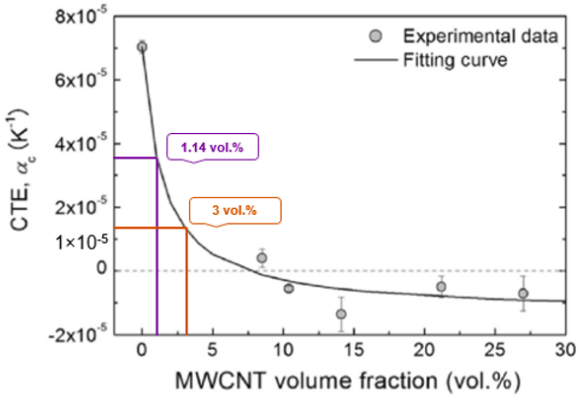

Figure 12. CTE with 1.14 vol% and 3 vol% MWCNTs [8]

1. The pre-existing defects in MWCNTs as was observed in the Raman Spectroscopy of the MWCNTs in the present study. The defects deteriorated the properties of the MWCNTs. Hence, the CTE of the polymer was not significantly decreased compared to the predicted theoretical CTE.
2. The catalyst used for the production of MWCNTs in the lab was Ferrocene during the chemical vapour deposition process. It was not possible to separate the catalyst from the MWCNTs. Therefore, the weight percentages of the MWCNTs used in the specimens were possibly less than the expected weight percentages. The catalyst did not contribute to the reduction of the CTE of the polymer [19].
3. There was a deviation on the density of MWCNTs used in the analytical calculation, as there was no effective method to measure the density of MWCNTs. The density of MWCNTs is related to the dimension of carbon nanotubes and the quantity of the walls in carbon nanotubes [20]. The diameter of the MWCNTs synthesised in the present study was between 20 nm-100 nm. The density of MWCNTs used in the present study might be under-estimated as the density of the MWCNTs varies from 1.5 gm/cm^3 to 2.5 gm/cm^3 [21].
4. The agglomeration occurs spontaneously because of the static conduction, consequently the re-agglomeration happened after curing, as shown in Figure 9. CNTs agglomeration induces a negative influence on the performance of polymer [16]. Agglomerates may work as initiation sites for failure or accelerate the final breakage.
5. The defects (porosity, void etc.) in the adhesive part of the specimens may cause poor bonding between the metal substrate and adhesive, which in turn can result different thermal expansion of the specimens. In the present study such defects were identified, see Figure 13. Insufficient degassing of the uncured epoxy causes formation of porosity and voids.

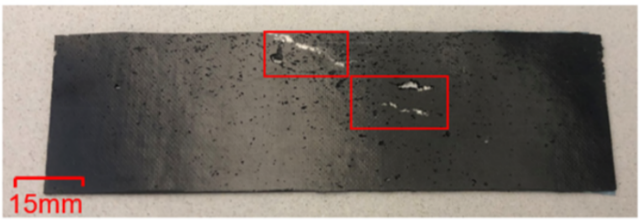

Figure 13. Defects on specimen, porosity (black features on the surface) and void (highlighted with red boxes)

Preprints (www.preprints.org) | NOT PEER-REVIEWED | Posted: 30 October 2020 doi:10.20944/preprints202010.0645.v1

4. Conclusions

The aim of the present study was to reduce the coefficient of thermal expansion (CTE) of an epoxy adhesive with the addition of multi walled carbon nanotubes (MWCNTs) in order to reduce the CTE mismatch in adhesive-metal bonded joint systems. A low viscosity bisphenol-A epoxy resin was modified with the addition of 1 wt% and 2.68 wt% MWCNTs and was used in adhesive-metal bonded joints. The MWCNTs was synthesised in the laboratory and the MWCNTs were assessed using Raman spectroscopy. Significant amount of defects was observed in the MWCNTs. The dispersion quality of the MWCNTs in the epoxy was examined using scanning electron microscopy (SEM). The MWCNTs were agglomerated i.e. poorly dispersed in the epoxy. The CTE of the adhesive-metal bonded joint was determined experimentally using thermal strain measurement technique. The addition of 1 wt% and 2.68 wt% of multi-walled CNTs (MWCNTs) decreased the CTE of the polymer adhesive from $7.5 \times 10^{-5}\ ^{\circ}C^{-1}$ (pristine level) to $5.87 \times 10^{-5}\ ^{\circ}C^{-1}$ and $4.43 \times 10^{-5}\ ^{\circ}C^{-1}$, respectively by 22% and 41% reduction. The reduction in the CTE was predicted theoretically which showed that CTE should have been reduced to $3.6 \times 10^{-5}\ ^{\circ}C^{-1}$ (52% reduction) and $1.4 \times 10^{-5}\ ^{\circ}C^{-1}$ (81% reduction). The discrepancy between the experimental and the theoretical values was caused by the above mentioned defects in the MWCNTs and the agglomeration of the MWCNTs in the adhesive. Moreover, porosity and voids were observed on the surface of the adhesive part of the adhesive-metal bonded joints. These defects of the adhesives may result in poor bonding between the metal and the adhesive, hence the discrepancy of the experimental and the theoretical CTE.

Author Contributions: X. Z. has carried out the experimentation, and established the first thesis of the results and discussion; T.K. has extracted the first draft of the current paper, and carried out critical and elaborative analysis of the data; H.Y.N, V.K.T. and I.A. have managed and supervised the multidisciplinary research in different areas; H.Y.N has introduced the first concept of the idea the article presents.

Funding: This research was funded by Engineering and Physical Sciences Research Council (EPSRC)

Acknowledgments: The authors would like to acknowledge supports from the UK EPSRC funded research (STRAINcomp; Ref. EP/R016828/1). The authors are also grateful to Mr. Jim Hurley and Mr. Ben Hopper from Cranfield University for strong and continuous technical supports throughout the research.

References

1. VENEDO (2019) Global EV Sales for 2018, http://www.ev-volumes.com/country/total-world-plug-in-vehicle-volumes/
2. Nezhad H. Y., Egan B., Merwick F., McCarthy C.T. Bearing damage characteristics of fibre-reinforced countersunk composite bolted joints subjected to quasi-static shear loading, Composite Structures. *Composites Structures* **2017**, *166*, 184-192.
3. Zhou Y., Nezhad H.Y., Hou C., Wan X., McCarthy C.T., McCarthy M.A. A three dimensional implicit finite element damage model and its application to single-lap multi-bolt composite joints with variable clearance, *Composites Structures* **2015**, *131*, 1060-1072.
4. Egan B., McCarthy C.T., McCarthy M.A., Gray P.J., O'Higgins R.M. Static and high-rate loading of single and multi-bolt carbon–epoxy aircraft fuselage joints, *Composites Part A: Applied Science and Manufacturing* **2013**, *53*, 97-108.
5. Long, Li. Research on Static Strength Analysis and Strength Prediction of Adhesively Bonded Single Lap Joint for Autoclave. *Ji Lin University* **2011**
6. GPC Battery (2015), http://www.gpcbattery.com/English/index.aspx
7. CBEA. Thermal Management of Electric Vehicle. *SAE Technical Papers* **2019**
8. Shirasu K., Yamamoto G., Tamaki I., Ogasawara T., Shimamura Y., Inoue Y., Hashida T. Negative axial thermal expansion coefficient of carbon nanotubes: Experimental determination based on measurements of coefficient of thermal expansion for aligned carbon nanotube reinforced epoxy composites. *Carbon* **2015**, *95*, 904-909.
9. Huntsman (2012), Mechanical Properties: Araldite ® LY 1564 / Aradur ® 3486 / Aradur ® 3487, http://www.swiss-composite.ch/pdf/t-Araldite- LY1564-Aradur3486-3487-e.pdf

10. Rojas J.A., Ardila-Rodríguez L.A., Diniz M.F., Gonçalves M., Ribeiro B., Rezende M.C. Optimization of Triton X-100 removal and ultrasound probe parameters in the preparation of multiwalled carbon nanotube buckypaper. *Materials and Design* **2019**, *166*, 107612.
11. Bai Y., Lin D., Wu F., Wang Z., Xing B. Adsorption of Triton X-series surfactants and its role in stabilizing multi-walled carbon nanotube suspensions. *Chemosphere* **2010**, *79(4)*, 362-7.
12. Ikeda H., Iwai M., Nakajima D., Kikuchi T., Natsui S., Sakaguchi N., Suzuki R.o. Nanostructural characterization of ordered gold particle arrays fabricated via aluminum anodizing, sputter coating, and dewetting. *Applied Surface Science* **2019**, *465*, 747-753.
13. Costa S., Borowiak-Palen E., Kruszyńska M., Bachmatiuk A., Kaleńczuk R. J. Characterization of carbon nanotubes by Raman spectroscopy. *Materials Science Poland* **2008**, *26(2)*, 433-441.
14. Epsilon (2019) MODEL LE-05 and LE-15 Non-Contact Laser Extensometer, `https://www.epsilontech.com/wp-content/uploads/product- specs/Laser-Extensometer.pdf`
15. Davis C.S., Woodcock J., and Gilman, J. Preparation of Nanoscale Mutli-walled Carbon Nanotube Dispersions in a Polyetheramine Epoxy for Eco-Toxicological Assessment. *Materials Science* **2015**, *26(2)*, 433-441.
16. Nezhad, H.Y., Thakur, V.K. Effect of Morphological Changes due to Increasing Carbon Nanoparticles Content on the Quasi-Static Mechanical Response of Epoxy Resin, *Polymers* **2018**, *10*,1106.
17. Bregar, T., An D., Gharavian, S. et al. Carbon nanotube embedded adhesives for real-time monitoring of adhesion failure in high performance adhesively bonded joints, *Scientific Reports* **2020**, *10 (16833)*.
18. An D., Nourry J., Gharavian S., Thakur V.K., Aria I., Durazo-Cardenas I., Khaleque T., Nezhad H.Y., Strain self-sensing tailoring in functionalised carbon nanotubes/epoxy nanocomposites in response to electrical resistance change measurement, 9th International Conference on Through-life Engineering Service 3-4 November **2020**, Cranfield UK.
19. Esquenazi G.L., Brinson B.E., and Barron A. Catalytic Growth of Carbon Nanotubes by Direct Liquid Injection CVD Using the Nanocluster [HxPMo12O40H4Mo72Fe30(O2CMe)15O254(H2O)98-y(EtOH)y]. *Materials Science* **2018**, *4(1)*, 17.
20. ELaurent Ch., Flahaut E., Peigney A. The weight and density of carbon nanotubes versus the number of walls and diameter. *Carbon* **2010**, *48(10)*, 2994-2996.
21. Mazlan, N.B. The effect of oxidation treatment of MWCNT on the properties of PDMS nanocomposite. PhD . *Sains Malaysia University* **2012**.